한국환경과학회지 제5권(제5호), 619~633, 1996
J. of the Korean Environmental Sciences Society

The 40~50Day Intraseasonal Oscillation of the Geostationary Meteorological Satellite High Cloud Amount

Kyung-Ja HA, Ae-Sook SUH*, Yasuhiro Sugimori, Ja-Yeon MOON**
*Research Institute of computer and information-communication, and Department of Atmospheric Sciences, Pusan National University, Pusan 609~735, Korea and Remote Sensing Lab., Meteorological Research Institute, Seoul 110~360, Korea**
*School of Marine Sciences & Technology, Tokai Univ., Shizuoka 424, Japan***
(Manuscript received 13 June 1996)

Intraseasonal variability of the tropical convection over the Indian/western Pacific is studied using the Geostationary Meteorological Satellite high cloud amount. This study is directed to find the tropical-extratropical interaction in the frequency range of intraseasonal and interannual variabilities of the summer monsoon occured over the domain of 90E-171W and 49S-50N. Especially, in order to investigate the intraseasonal interaction of East Asia summer monsoon associated with the tropical convections in the high cloud amounts, the spatial and time structure of the intraseasonal oscillation for the movement and the evolution of the large-scale convections are studied.

To describe the spatial and the time evolution, the extended empirical orthogonal function analysis is applied. The first mode may be considered to a normal structure, indicating that the strong convection band over 90E-120E is extended to eastward, but this mode was detected as a variable mode near Korea and Japan. The second, third and fourth modes were amplified with the intraseasonal variability during summer monsoon. It is found that the dominant intraseasonal mode of the tropical convection consists of the spatial changes over a broad period range centered around 40~50days.
Key words :

1. INTRODUCTION

It is well known that heat sources in the tropical oceans play an important role in general circulations of the global atmosphere. Heat sources in the tropics are mostly resulted from the release of latent heat distributed according to the spatial and temporal variations of rainfall over the earth. However, reliable estimate of spatial distribution of precipitation in the tropical oceans is quite difficult because of sparseness of surface observation stations. Diagnostic methods to estimate rainfall amount by using the meteorological satellite image data have been developed in the studies of Barnett (1970), Kilonsky and Ramage (1976), Maruyama *et al.* (1986) and many others. Recently, for monitoring the tropic rainfall regime, the TRMM (Tropical Rainfall Measuring Mission) has been proposed (Simpson *et al.*, 1988). As the cloud amount determined hourly from the Geostationary Meteorological Satellite (GMS) infrared observations is produced for the land and ocean surfaces, it is very important products to investigate the locations and strength of precipitation band associated with frontal convergence over East Asia in summer. Thus, it can be confirmed that the results from analysis of this high cloud amount shows the detailed seasonal migrations of the convective zone in its strength and position of the summer monsoon cloud.

In this study, the interannual variabilities and intraseasonal oscillations in the five day mean and monthly mean fields of the high cloud amount over the summer monsoon regions of Asia such as South Asia and East Asia will be investigated. In recent years, the quasi periodical phenomena

called 40~50day oscillation have become the key point for studying of the intraseasonal variability of the tropical atmosphere since the pioneering work of Madden and Julian (1971, 1972). The 40~50day oscillation is the strongest low-frequency signal up to the present in the tropical atmosphere. Its potential implication on long-range weather forecast and short-term climate prediction may be significant. Yasunari (1980) and Maruyama (1982) reported the existence of quasi 40day cloudiness oscillations over the summer monsoon region of East Asia and India. All of the above works were based on observation data limited in space and time in many respects.

The global nature of the 40~50day oscillation has been revealed in the studies of long-term records carried out by Weikmann *et al.* (1985), Knutson *et al.* (1986), and Lau and Chan (1986, 1988). From the theoretical treatments of Lau and Peng (1987) and Sui and Lau (1989), the origin and the propagation mechanism of low-frequency intraseasonal oscillations in the tropical atmosphere has been proposed by Kang *et al.* (1989) who emphasized the 30~60day oscillation appearing in the climatological variation of outgoing longwave radiation over East Asia during the summer time. Their result shows that more than 40% of the climatological variation during summer is composed with the time scale of 30~60days over the subtropical western Pacific. Nakazawa (1992) studied seasonal phase lock of intraseasonal variation during the Asian summer monsoon using 12-year OLR data. From his study, he found that the enhancement of Asian summer monsoon activity occurs intermittently with a period of 30~60days, and are in general phase locked with annual march of the seasonal cycle. Ueda *et al.* (1995) investigated abrupt seasonal change of the activity of large-scale convections over the western Pacific in the Northern Hemisphere summer time.

In this study, major analysis focus on investigation the intraseasonal and interannual variabilities of the structure of summer monsoon with large-scale convection, and the characteristics of intraseasonal oscillation and it's variability are analysed as important process showing tropical-extratropical interaction. And this study is guided by the results of analysis of large-scale low-frequency variability, of tropical western Pacific convective cloud based on an empirical orthogonal function analysis, and of extratropical convection variability.

2. The GMS high cloud amount

2.1 The mean fields

The GMS cloud has been retrieved by 1°×1° grid data over the region of 49S-50N and 90E-171 W originally. The low and high cloud amount have been retreived by threshold and multi spectral statistical techniques, the total cloud amount by summation of low and high clouds, their 5-day mean and monthly means have been achieved.

The high and low, cloud and no cloud decision made from the threshold temperature. The threshold temperature used in decision high and low cloud was obtained from the vertical profile predicted by numerical weather forecasting division. That is, the high cloud amount which is expressed as the percent of the total grid area is defined as the clouds with a cloudtop temperature below the 400 hpa level analyzed temperature based on the upper air observations. Hence the comparison between the Intertropical Convergence Zone and the Baiu ¼or Mei-yu¾ front is much easier to make than with commonly-used OLR data.

The high cloud amount used in this study are represented by 50×50 grid data of the five-day mean 2-degree latitude-longitude grid over the domain of 49S-50N and 90E-171W. The data includes 73-pentad in one calendar year.

The period of data analysis was divided into two parts, because no data over the land are available prior to March 1987. One part is the periods from January 1979 to February 1987, the other one part is the periods from March 1987 to December 1994.

2.2 High cloud amount climatology

The climatological mean monthly value is calcu-

lated from 8-year high cloud amount that are available over the land and the ocean.

It is well known that the monsoon convection possesses many different time scales. This means that the climatology of the monsoon convection cannot be appropriately described by simply taking the harmonic mean. First of all, the 5-day climatology can be obtained by averaging the corresponding 8-year periods of 1987~1994 over the analysis regions. Figure 1 represents the wintertime (Dec.-Feb.) and summertime (Jun.-Aug.) mean high cloud amount averaged for eight-year. This figure shows that the summertime convection is active in 10N latitude band of the equatorial regions and 30-40N latitude of East Asia regions including China, Korea, and Japan.

Figure 2 shows the cross section for eastern Asia of 120-130E. The most conspicuous feature is the monsoon onset between 25N and 30N as indicated by the steep increase in high cloud amount starting from 26th pentad (6May~10May) and 31th pentad (31May~4June), respectively. The maximun value found near 34th pentad (15June~19June) corresponds to the onset of the Mei-yu (changma or Baiu) in East Asia. After the Mei-yu onset is fully established, the maximum band propagates northward to about latitude 40N, while the southern latitudes begin to dry out. Standard deviation (lower panel) are large at regions with the large cloud value. And it is also large near 20N at the time roughly coincides with occurring the maximum convection. The large standard deviation can be interpreted by the strong interannual variation.

Figure 3 shows the high cloud amount from the equator to 50N averaged over 120E-172W. The north-south excursion of Asian monsoon from 30N to 40N convection is well observed for the summer period of 1987~1994 except from 1979~1986. The relatively weak excursion for 1979~1986 is due to missing of the land-based data. In a broad sense, this Asian summer monsoon convection related to the extension of the monsoon trough or Mei-yu rain band over East Asia and the north-western

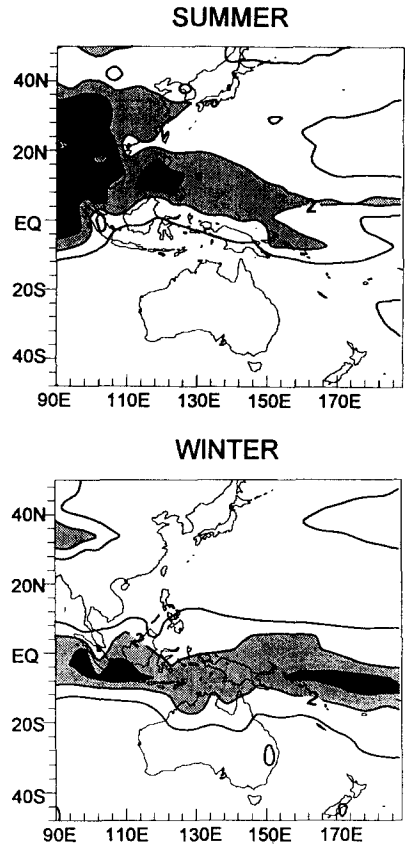

Fig. 1. (a) The summertime and (b) wintertime mean of GMS high cloud amount (1987~1994).

Pacific. It can be realized that the interannual variabilities of the Intertropical Convergence Zone of the Asian rainband are basically resolved by analysis of the 5-day mean GMS high cloud amount.

3. The intraseasonal oscillation and its interannual variabilities

3.1 The Interannual and intraseasonal variances

The total variance for 8-year period (1987~1994) may be decomposed conveniently into the variance of annual means and the annual variances over the period. In this study, to present the variance distribution of the 5-day mean high cloud amount, IAV (interannual variance) and ISV (intraseasonal variance) are calculated similar to Lau

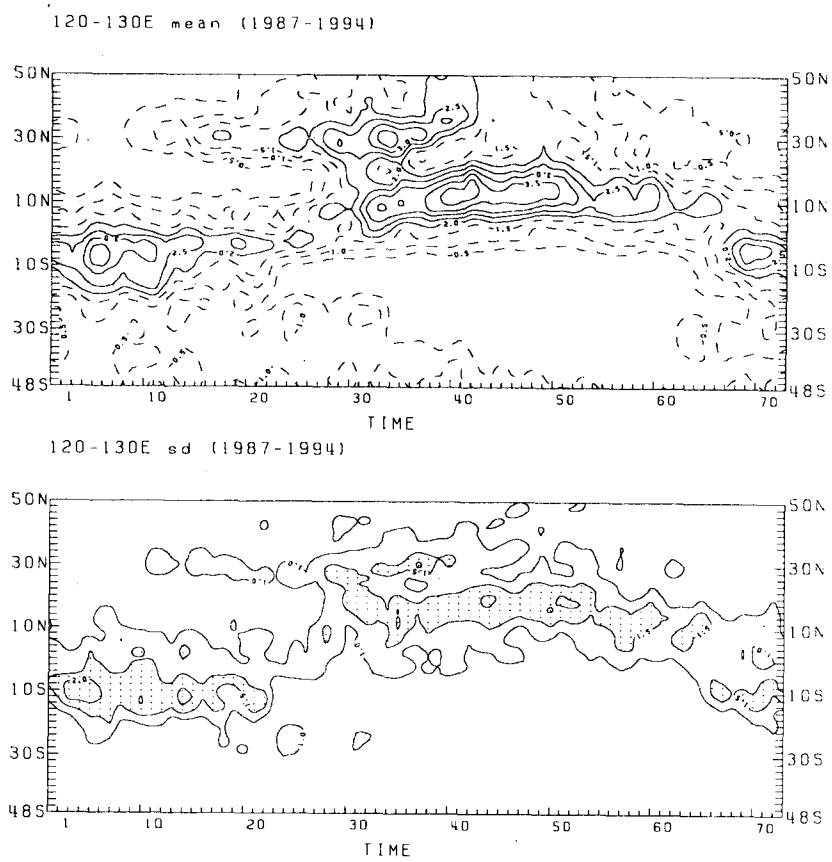

Fig. 2. Annual march of SST emerged from the average of the eight-year means (upper panl) and standard deviations (lower panel) of the five-day mean high cloud amounts along the longitudinal strip confined within 120E and 130E. In the upper figure the negative contours are dashed. And the area with values larger than or equal to 1.5 are shaded in the lower figure.

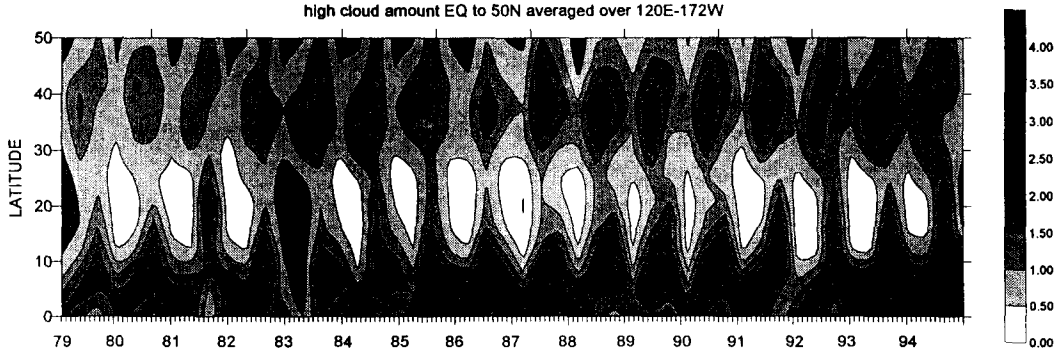

Fig. 3. Latitude-time section of GMS high cloud amount averaged over 120E-172W.

and Chan (1988). The IAV variance is defined as

$$LAV = 1/J \sum_{j=1}^{J} \overline{X}_j^2 \qquad (1)$$

where J stands for the total number of years and X_j the 37 pentad anomaly for

the j th year. The ISV for J year is computed as

$$ISV=1/J\sum_{j=1}^{J}(1/I\sum_{j=1}^{I}(X_{ij}+\overline{X}_j)^2) \quad (2)$$

Where I (=37 from 1 April to 2 October) is number of petagons. That is, the i is the pentad index. Thus, the total anomaly variance is defined as the sum of IAV and ISV. All the variance estimates to be discussed in this study are computed using deviations from the seasonal cycle.

Figure 4 shows the interannual components of summertime variances. The interannual component for six months (April -September) high cloud amount variation is concentrated in the tropical Indian Ocean, and central Pacific, where the Nino event is concentrated. However, the maximum of the interannual component of three months (June-August) of summertime high cloud amount variation is divided by the tropical band, the higher latitude band of 25N-35N, and the subtropical western Pacific.

Figure 5 shows the intraseasonal component of the summertime high cloud amount variance. The intraseasonal variance patterns of six months of April-September and three months of June-August are similar, and represented the maximum over the Asia land and near the South China Sea. Com-

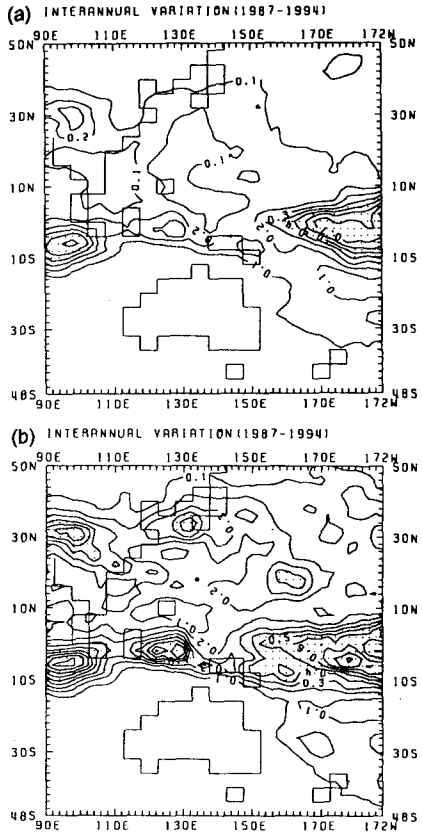

Fig. 4. Interannual component of the (a) summertime (April-September) and (b) summer (June-August) high cloud amount variance.

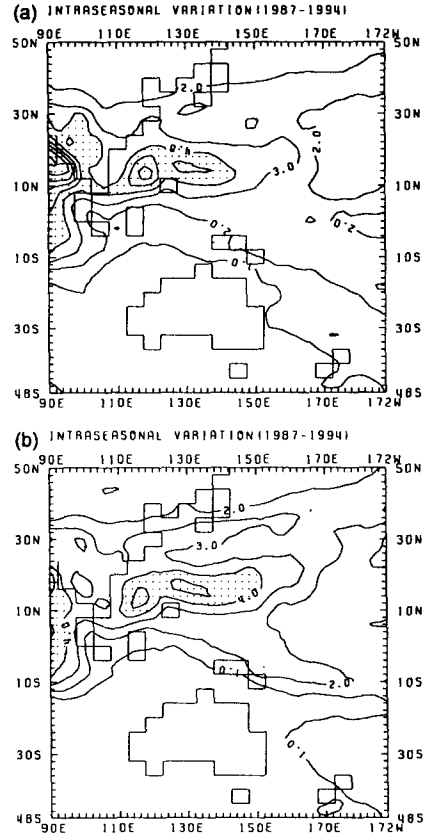

Fig. 5. Intraseasonal component of the (a) summertime (April-September) and (b) summer (June-August) high cloud amount variance.

parison of ISV with the corresponding climatological seasonal mean in Fig. 1 reveals that areas with large variance coincide with areas of high mean high cloud amount. In this figure the eastward extensions of high convection in equatorial and in latitude of 30N-40N can be realized. There are pronounced subtropical minimum over the central Pacific. This minimum represents the relative lack of convective activities over the subtropical oceanic "dry" zone.

To obtain the relationship between the tropical convective oscillations and East Asia summer monsoon convection, firstly, longitudinal and time sections of high cloud amount at constant latitude are represented as Fig. 6. From Fig. 6, it can be realized that the high cloud amount derived from GMS is very similar to the observed rainfall from Lau et al. (1995). The 1982/1983 El Nino and 1987 El Nino and 1988/1989 La Nina pattern are well exposed by eastward propagation to central Pacific. Especially the strong rainfall and strong high cloud amount have the consistent pattern. It shows that the climatology of high cloud amount derived from satellite can be a good index to equatorial precipitation.

3.2 The 40~50 day intraseasonal oscil-

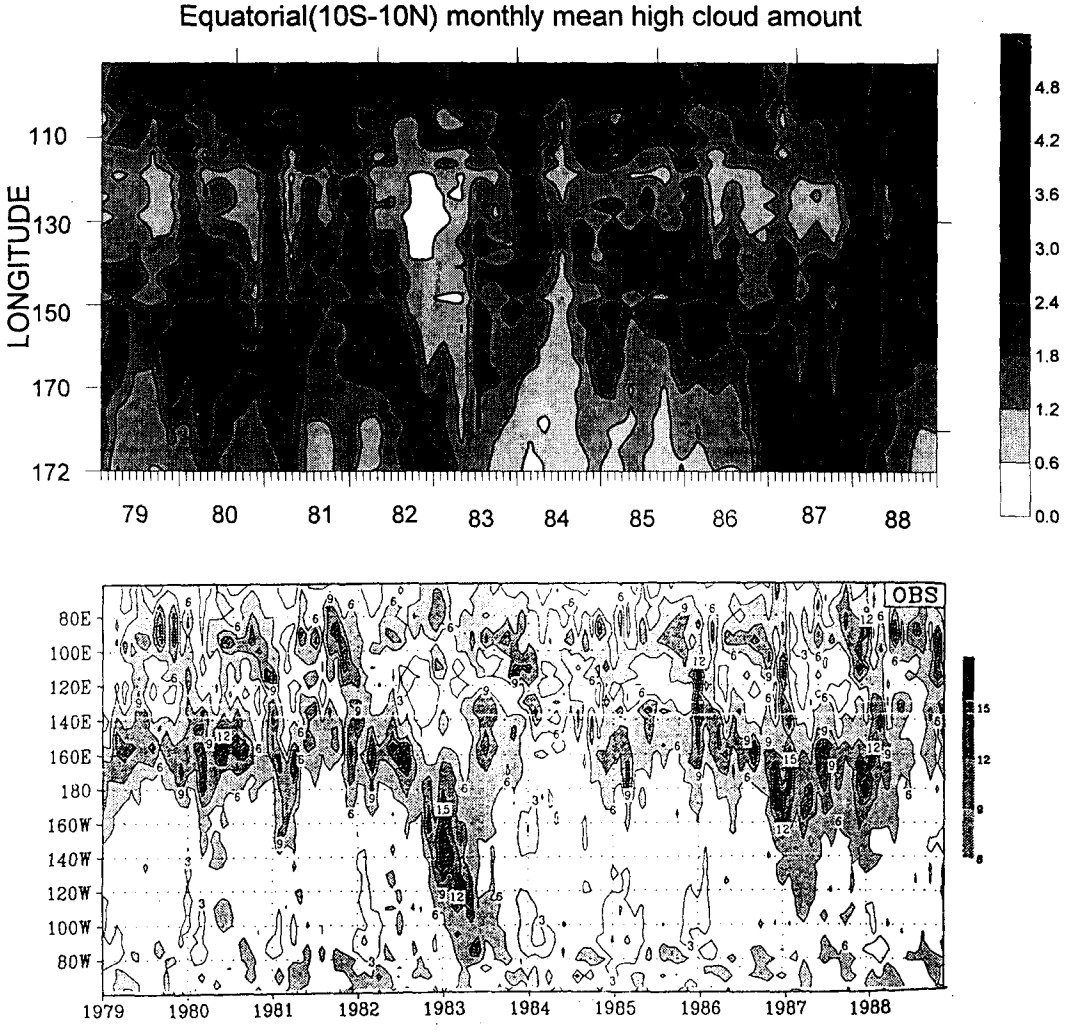

Fig. 6. The longitude-time section of the equatorial (10S-10N) monthly mean high cloud amount.

lation

Since there is evidence of the coexistence of different time scales in the variation of convective activity, we have employed the technique of spectral analysis of high cloud amount as a function of the time-space distribution as a tool for the extraction of periodicity.

In order to demonstrate the apparent periodicity in the tropical convective oscillation, the selected regions were formed in the zonal band from equator and 20N.

In order to obtain the apparent periodicity the spectrum analysis was performed with Parzen spectral windows $\omega_n(\theta$ (Priestley, 1981).

$$W_n(\theta)=\frac{6\pi}{M}[F_{M/2}(\theta)]^2\{1-\frac{2}{3}\sin^2\left(\frac{\theta}{2}\right) \quad (3)$$

where

$$F_{M/2}(\theta)=\frac{1}{\theta M}\left[\frac{\sin\frac{M\theta}{4}}{\sin(\frac{\pi}{2})}\right]^2 \text{ and } M=30. \quad (4)$$

Spectral method is applied to the entire data period of approximately 16 years of 5-day mean high cloud amount at regions of 10×10 degrees along the tropical band from equator and 20N. To determine the intraseasonal oscillation, the smooth seasonal cycle of each year must be obtained. Since it is unclear how many harmonics are required to accurately describe the seasonal cycle, we shall adopt the smoothed curve by fitting with 3rd polynomial function along the pentad day.

Spectra for selected grid points are shown in Fig. 7 It is seen that peaks in the spectra in the 40~50 day range (referred to as the 40~50 day signal) are mostly confined to the tropical areas west of the 120E.

Along the equator the signal is most pronounced over the Indian Ocean and western Pacific west of 120E, but over the east of 120E the signal drops off very rapidly. Near the date line, the 40~50day signal appears again, while the signal becomes very much weakened. The region of most strong 40~50 day coincides with the center of strong intraseasonal convective activities during the northern summer (Lau and Chan, 1986). But in area of 120 E-140E the intraseasonal oscillation near 40~50day appears as the second peak at 10-20N rather than the tropical ocean. From these analysis, it is noteworthy that the 40~50day in 120E-140E is changed to the northward. This is similar to Murakami et al. (1986)'s result that found the 45-day transient waves are not purely propagating character, they tend

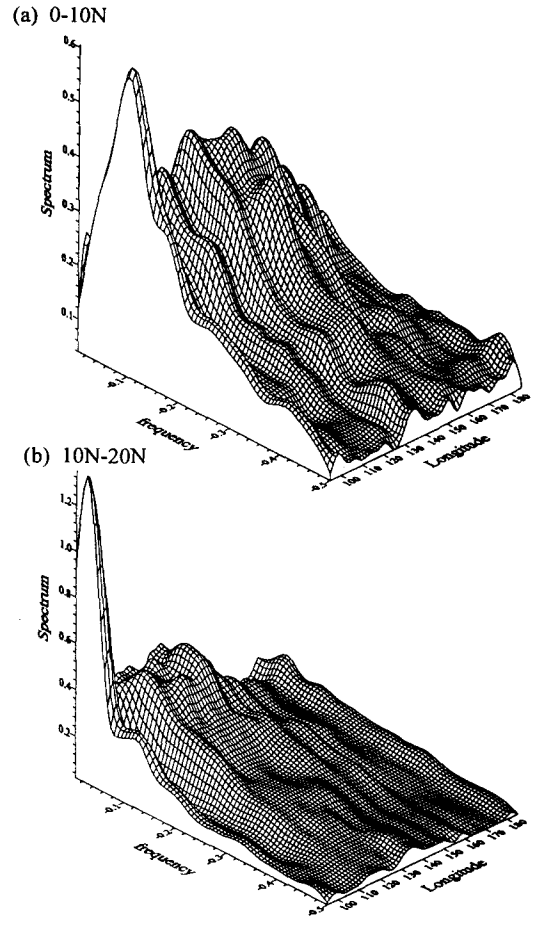

Fig. 7. Spectral density function of the domain averaged (10/10 degree lat/lon) high cloud amount in (a) 0-10N and (b) 10 N-20N.

to dramatically intensify when passing through the eastern Indian and western Pacific oceans, a feature similar to standing waves with monsoonal effects acting as the major regulator of the 45-day transients. That is, at 10N and 20N between the Indian and the western Pacific, 40~50day signals are found although they are not uniformly significant over this region. We can also recognize from this results that the relationship between the intraseasonal oscillation and monsoon onset in the Northern summer hemisphere may be realized by activity of intraseasonal oscillation in the western Pacific.

In order to explain the movement processes that exhibits a northward propagation across the western Pacific, the time-lag evolution of systems developing and moving eastward, and moving westward must be investigated. Zhu and Wang (1993) also emphasized that there are the summertime convective seesaw results from a time-lag evolution of these systems.

3.3 The principal structure of the intraseasonal oscillation

There are so many studies which identify the 40~50 day oscillation and its relationship with ENSO. Among the studies, especially Murakami and Nakazawa (1985) pointed out that the summer monsoon onset and the active/break cycle in the Northern hemisphere summer are closely related to the global eastward propagation of the 40~50 day oscillation. The relationship between the 40~50 oscillation and ENSO can be known from the year by year characteristics.

In this study, the yearly characteristics for time evolution of the intraseasonal oscillation is analyzed from the principal mode analysis with extended empirical othogonal functions.

The principal modes of deviation fields will be expressed by the eigenvectors and their associated series of coefficients (hereafter called coefficient series for brevity) that belong to the largest four eigenvalues of the symmetric matrix of I×I elements, which are the normalized covariance between pairs of departures for 37-pentad data.

Moreover, in order to investigate characteristics of time evolution of the principal spatial structure, extended empirical orthogonal function (EEOF) analysis with the window size of 37-pentad (185 days) is applied to each year. The window size is decided by judgement that the 37-pentad can include the seasonal scale, and then the structure in

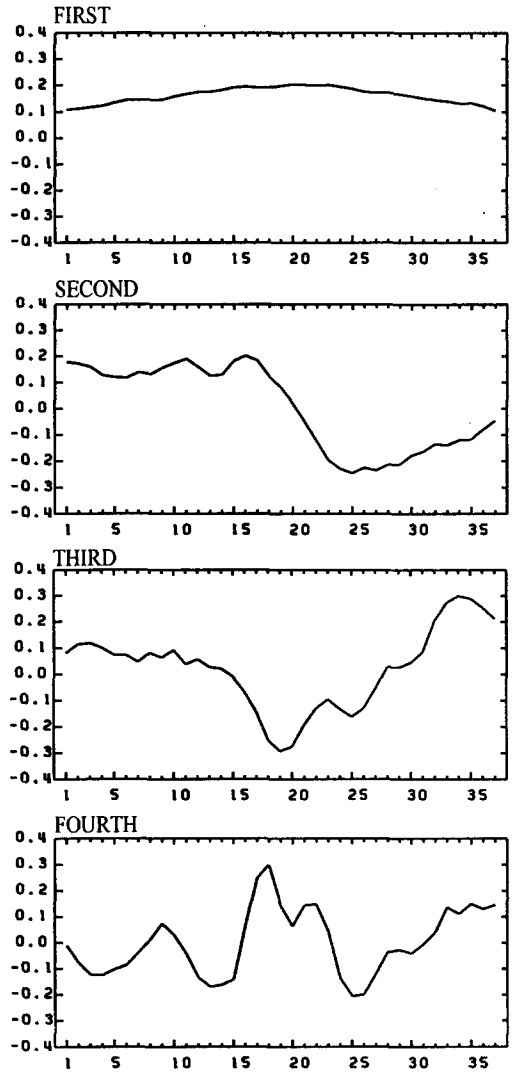

Fig. 8. The first four principal components resulted from the EOF analysis of eight-year summertime GMS high cloud amount over East Asia region.

window explains the normal character. That is, to demonstrate the yearly characteristics, we used one summertime, 37-pentad window size.

Now we can convert the original time-spatial function μ_{ij} of high cloud amount to new time-spatial function $\mu_{ij'}^{(n)}$ reconstructed by which n is the number of windows. Then, $\mu_{ij'}^{(n)}$ can be expressed by the sum of the products of the time variation function, $\Psi_{j'l}$ and the space variation functions, $\mu_{ij'}^{(n)}$ as following formula.

Therefore, $\mu_{ij'}^{(n)}$ is consisted of time function by spatial function.

$$\mu_{ij'}^{(n)} = \sum_{l=1}^{L} \alpha_{il}^{(n)} \Psi_{j'l} \qquad (3)$$

Where, α_{il} is the window averaged space structure with the weight being the l-theigenfunction. $\Psi_{j'l}$ is common time structure of windows, and can be determined as the eigenfunction of covarience matrix of $\mu_{ij'}$. Eigenvectors are represented as common time structure indicating the time variation within one window size.

Figure 8 and Fig. 9 show the common time structure of windows and the eight-window averaged space structure with the weight being the first four eigenfunction, respectively. Namely, Fig. 9 shows the yearly characteristics of spatial structure, being taken with common temporal structure of the first four principal modes of the EOF analysis. The

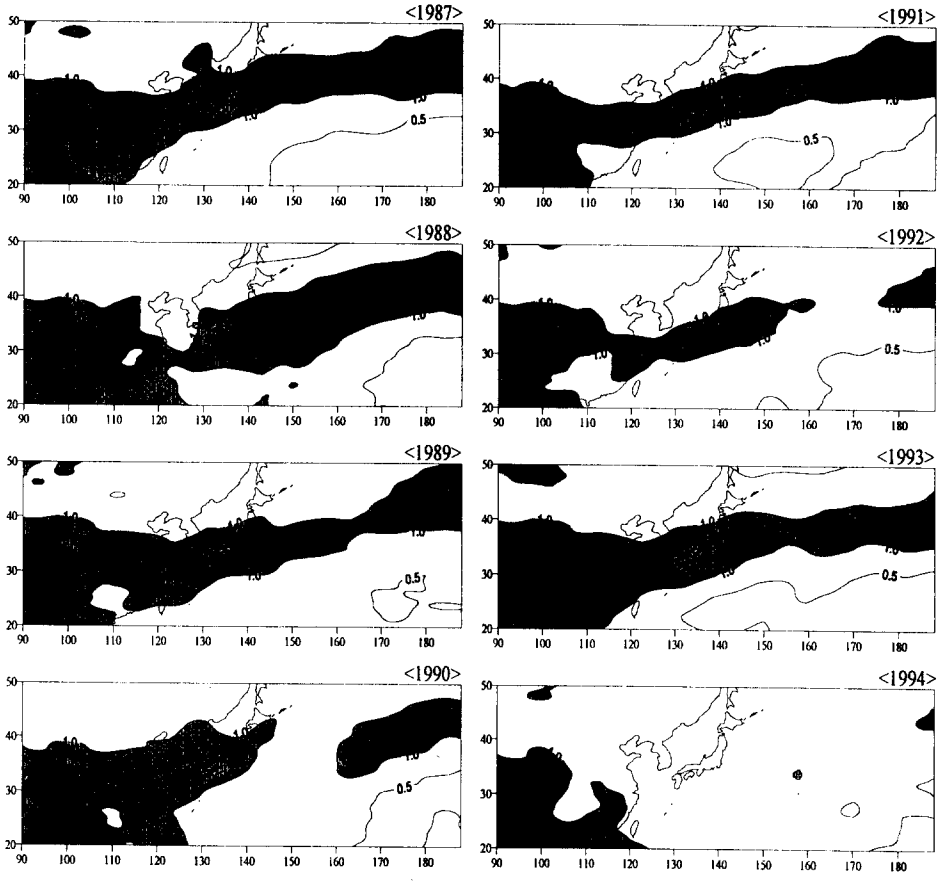

Fig. 9. The spatial structures of the first four principal components of the EOF analysis. The numbers from 1 to 8 mean 1987~1994.
Contour interval is 0.5. Negative valued contours are dashed. The ared with larger values than 1.0 are dark shaded and those with less than -1.0 are lightly shaded.

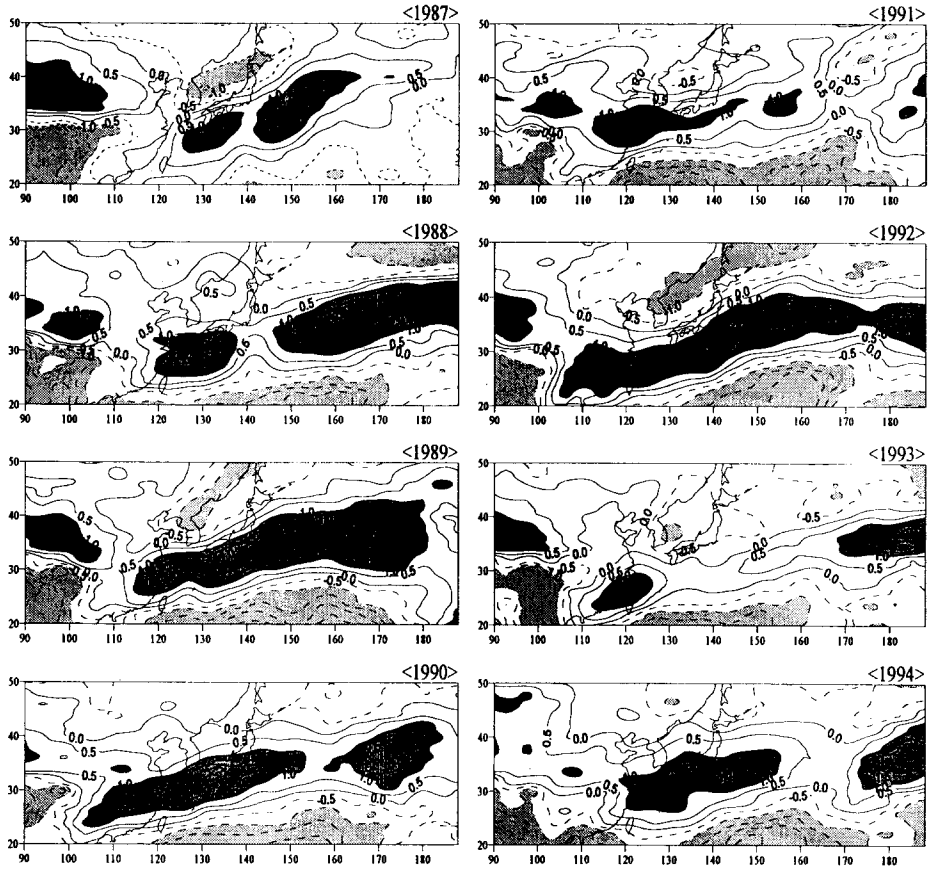

Fig. 9 continued

numbers from 1 to 8 mean 1987~1994. Countor interval is 0.5. Negative valued contours are dashed. The area with larger values than 1.0 are dark shaded and those with less than -1 are lightly shaded. The values in each mode is normalized. So the actual magnitude of variability can be estimated by multiplying the values of the principal modes shown in Fig. 8 to the values in this figure.

The first principal mode (solid line) explains the most of variability over 64% of mean total variances for summertime of eight years. This EEOF first mode exhibits relatively seasonal variation or quasi-stationary mode, while second, third and fourth represent intraseasonal modes as shown by Fig. 8 and Fig. 9.

From the first mode (the solid line in Fig. 8 and Fig. 9 (a)) we can realize that the strong convection band over 90E-120E is extended to eastward, and this eastward extension varies with year to year variation. Especially this first mode may be concidered to a normal structure, but this mode can de detected as variable mode near Korea and Japan. This eastward propagation of convection is weaker in 1991 and 1994 than another year. And in 1990 this propagation is ceased over East Asia region.

The second mode shows that the oscillation have a crest and a trough in one summertime. This mode is related to north-south transition of the zonally extended band of convection. Specially, it is shown at the spatial mode that the significant structure is represented over ocean near Japan and Korea, and at the temporal mode that the major pattern rapidly change near 20 pentad (5July~

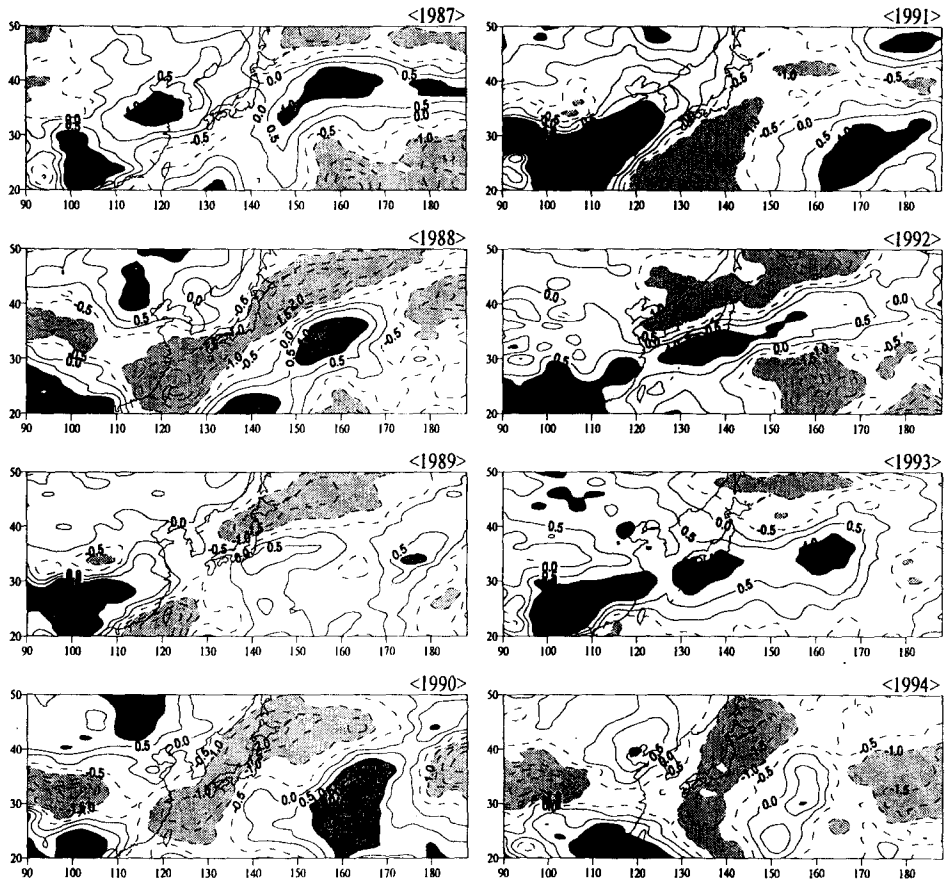

Fig. 9 continued

9July). The intensity of the second mode is also different from year to year. In 1988, 1990, 1991 and 1994 there are approximately similar patterns near Korea.

From third mode, the intensity is strongest in July and the periodicity is about 30~40day. This pattern is stretched from southwest to northeast over the edge of north Pacific high in summertime. This mode is important intraseasonal oscillation associated with the intensity of north Pacific high.

The fourth mode has two peaks in center of summer season, and has approximately 20-day period. This mode may be also considered as intraseasonal oscillation related to monsoon convection over East Asia. It is represented that the significant pattern is concentrated near Korea. Particularly, an abrupt northward shift of active convection is norticeable from 20N up to 40N.

In recent study of Nakazawa (1992), it has been reported that seasonal phase locking of intraseasonal variation is found during the Asian summer monsoon. The maximum intensity in the third and fourth modes of this analysis are in phase at the center (16th-23th pentad) of the summertime. This result can be considered as seasonal phase locking associated with the onset and break of East Asia summer monsoon.

4. Discussions and Conclusions

The evolution of high cloud amount for the period of 1979~1994 over the analyzed domain was investigated with some emphasis on the intraseasonal oscillation.

Especially, EEOF analysis is used to investigate

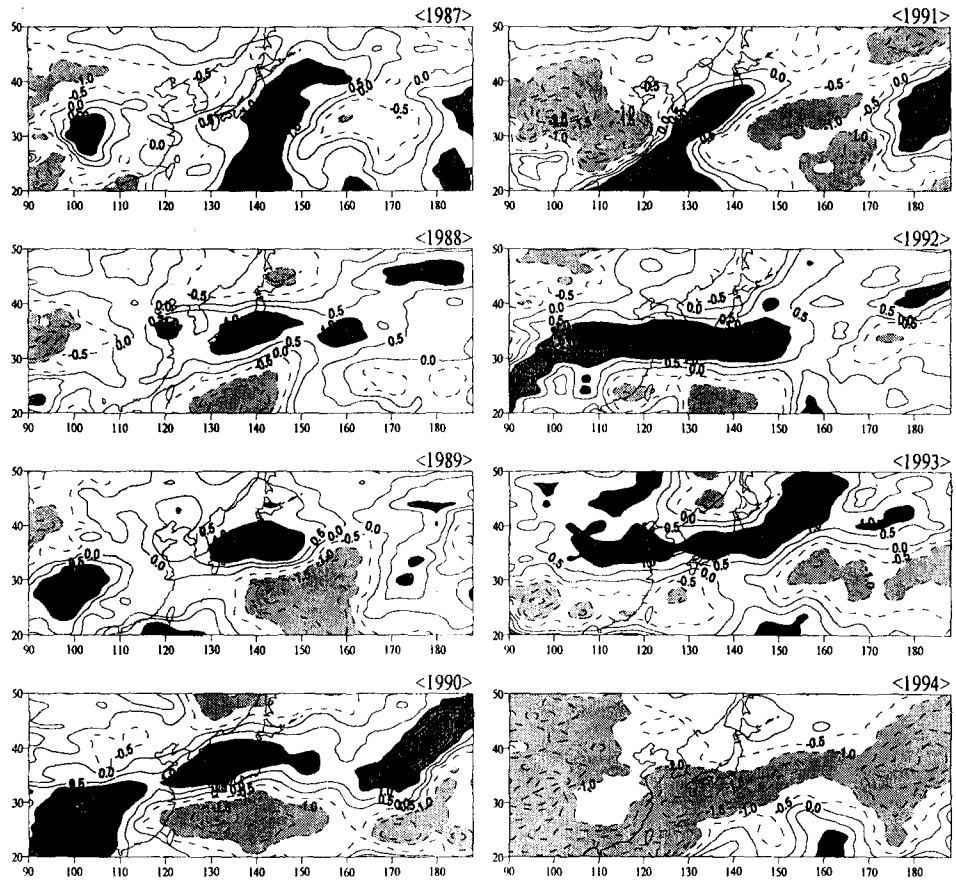

Fig. 9 continued

the principal char acteristics of time evolutional structure, and the spectral analysis is applied to obtain the periodicity of wave activity in equatorial Pacific region.

The major results obtained in this study can be summarized as follows. The most prevailing intraseasonal oscillations of GMS high cloud amount are longitudinally presented by the 40~50days mode, the 120days mode, and the 20days mode in the equatorial region. However it was found that the most prevailing modes over the equatorial western Pacific and Indian Ocean were different for each year, hence raising the possibility that the monsoon convectivity may be more fundamentally related to the interaction of intraseasonal oscillations and seasonal variation of convective over the lower latitude ocean. Particularly, the 40~50day oscillation showing the movement to northward in the western Pacific can be explained as the time-lag evolution of systems of eastward moving and westward moving.

From the principal mode analysis, the yearly characteristics of convective cloud pattern with common temporal variation during summertime was investigated. The first mode may be considered as a normal structure, indicating that the strong convection band over 90E-120E is extended to eastward, but this mode was detected as a variable mode near Korea and Japan. Particularly, the third and fourth modes were amplified with the intraseasonal variability of 40~50day and about 20day during summer monsoon. And they were related to stretching from southwest to northeast of convective cloud and abrupt northward migration of equa-

torial convective cloud band.

Acknowledgements

The authors wish to express many thanks to Prof. Gyu-Ho Lim in Seoul National University for his valuable comments on this study.

REFERENCES

Barnett, E. C., 1970: The estimation of monthly rainfall from satellite data. *Mon. Wea. Rev., 98,* 322~327.

Kang, I.-S., S.-I. An, C.-H. Joung, S.-C. Yoon and S. M. Lee, 1989: 30~60day oscillation appearing in climatological variation of outgoing longwave radiation around East Asia during summer. *J. Korean Meteoro. Soc., 25 (4),* 221~232.

Kilonsky, B. J. and C. S. Ramage, 1976: A technique for estimating tropical open-ocean rainfall from satellite observations. *J. Appl. Meteor., 15,* 972~975.

Knutson, T. R., K. M. Wickmann and J. E. Kutzbach, 1986: Global scale intraseasonal oscillations of outgoing longwave radiation and 250 mb zonal wind during northern hemisphere summer. *Mon. Wea. Rev.,114,* 605~623.

Lau, K. -M. and P. -H. Chan, 1986: Aspect of the 40~50day oscillation during the northern summer as unfered from outpoing longwave radiation. *Mon. Wea. Rev., 114,* 1354~1367.

Lau, K. -M. and L. Peng, 1987: Origin of low-frequency (intraseasonal) oscillations in the tropical atmosphere. Part 1:Basic theory. *J. Atmos. Sci., 44,* 950~972.

Lau, K. -M. and P. H. Chan, 1988: Intraseasonal and interannual variations of tropical convection: A possible link between the 40~50day oscillation and ENSO? *J. Atmos. Sci., 45,* 506~521.

Lau, K.-M., Y. C. Sud and J.-H. Kim, 1995: Intercomparison of hydrologic processes in global climate models. NASA Technical Momorandum 104617. NASA Goddard Space Flight Center. Madden, R. A. and P. R. Julian, 1971: Detection of a 40~50day oscillation in the zonal wind in the tropical Pacific. *J. Atmos. Sci., 28,* 702~708.

Madden, R. A. and P. R. Julian, 1972: Description of global scale circulation cells in the tropics with 40~50day period. *J. Atmos. Sci., 29,* 1109~1123.

Maruyama, y., 1982: Upper tropospheric zonal wind oscillation with a 30~50day period over the equatorial western Pacific observed in cloud movement vectors. *J. Meteor., Soc. Japan, 44,* 25~42.

Maruyama, T., T. Nitta and Y. Tsuneoka, 1986: Estimation of monthly rainfall from satellite-observed cloud amount in the tropical western Pacific. *J. Atmos. Sci., 62,* 88~108.

Murakami, T. and T. Nakazawa, 1985: Tropical 40~50day oscillations during the 1979 Northern Hemisphere summer. *J. Atmos. Sci., 42,* 1107~1122.

Murakami, T., L.-X. Chen and A. Xie., 1986: Relationship among seasonal cycles, low-frequency oscillations, and transient disturbances as revealed from outgoing longwave radiation. *Mon. Wea. Rev., 114,* 1456~1465.

Nakazawa, T., 1992: Seasonal phase lock of intraseasonal variation during the Asian summer monsoon. *J. Meteor. Soc. Japan, 70,* 597~611.

Priestley, M. B., 1981: Spectral analysis and time series, Vol.1 and 2, Academic Press, New york.

Simpson, J. A. Adler, R. F. and North, G. R., 1988: A Proposed Tropical Rainfall Measuring Mission (TRMM) satellite. Bull., Amer., Meteor. Soc., 69, 278~295.

Sui, C. H. and K. -M. Lau, 1989: Origin of low-frequency (intraseasonal) oscillations in the tropical atmosphere. Part II: Structure and propagation of mobile wave-CISK modes and their modification by lower boundary forcing.

J. Atmos. Sci., 46, 37~56.

Ueda, H., T. Yasunari and R. Kawamura, 1995: Abrupt seasonal change of large-scale convective activity over the western Pacific in the northern summer. *J. Meteoro. Soc. Japan*, 73, 795~809.

Weickmann, K. M., G. R. Lussky and J. E. Kutzbach, 1985: Intraseasonal (30~60day) fluctuations of outgoing longwave radiation and 250 mb streamfunction during northern winter. *Mon. Wea. Rev., 113*, 941-961.

Yasunari, T., 1980: A quasi-stationary appearance of 30~40day period in the cloudiness fluctuations during the summer monsoon over India. *J. Meteor. Soc. Japan, 58*, 225~229.

Zhu, B. and B. Wang, 1993: The 30~60day convection seesaw between the tropical Indian and western Pacific Oceans. *J. Atmos. Sci., 50*, 184~199.

GMS 상층운량의 40~50일 계절안 진동

하경자 · 서애숙* · 杉森康宏** · 문자연
부산대학교 컴퓨터 및 정보통신연구소, 대기과학과, 기상연구소 원격탐사연구실*, 일본 東海大學 해양학부**
(1996년 6월 13일 접수)

인도양 및 서태평양 부근의 적도 대류의 계절안 변동을 GMS 상층운량을 사용하여 연구되었다. 이 연구는 90E-171W와 49S-50N 영역에서의 여름 몬순의 계절안 및 경년 변동 주기내의 열대-중위도 상호관계를 찾는데 방향이 맞추어져 있다. 특히 상층운량에서 적도 대류와 연관된 동아시아 몬순의 계절안 상호작용을 이해하기 위해 대규모 대류의 이동과 진화에 대한 공간 및 시간 구조의 분석이 이루어졌다.

공간과 시간 발전을 동시에 보기 위해 연장 경험적 직교함수 분석이 적용되었다. 그 첫째는 정규 구조로 간주될 수 있는, 90E-120E의 강한 대류의 동쪽 확장이 뚜렷한 모드이나 우리나라와 일본 부근에서는 해마다 변동하는 모드이다. 둘째, 세째 및 네째 모드들은 여름 몬순 동안 계절안 변동성을 가지고 증폭되는 모드들이다. 적도 대류에서 가장 강력한 계절안 모드가 바로 40~50일 부근에 탁월 주기를 갖고 있는 공간 구조로 구성되는 것이 확인되었다.